Neurotoxicology 72 (2019) 1–5

Contents lists available at ScienceDirect

Neurotoxicology

journal homepage: www.elsevier.com/locate/neuro

Full Length Article

Difference in ability for extracellular Zn^{2+} influx between human and rat amyloid β_{1-42} and its significance

Haruna Tamano[a], Hiroki Suzuki[a], Shuhei Kobuchi[a], Paul A. Adlard[b], Ashley I. Bush[b], Atsushi Takeda[a,*]

[a] Department of Neurophysiology, School of Pharmaceutical Sciences, University of Shizuoka, 52-1 Yada, Suruga-ku, Shizuoka, 422-8526, Japan
[b] The Florey Institute of Neuroscience and Mental Health, The University of Melbourne, Parkville, VIC., 3052, Australia

ARTICLE INFO

Keywords:
Extracellular Zn^{2+}
Rat $A\beta_{1-42}$
Dentate gyrus
Long-term potentiation

ABSTRACT

The accumulation of amyloid-β_{1-42} ($A\beta_{1-42}$), a constituively-generated peptide, in the brain is considered an upstream event in pathogenesis of Alzheimer's disease. $A\beta_{1-42}$-induced pathophysiology has been extensively studied in experimental mice and rats. However, neurotoxicity of murine $A\beta_{1-42}$ is much less understood than human $A\beta_{1-42}$. Here we report difference in ability for extracellular Zn^{2+} influx into dentate granule cells of rats between human and rat $A\beta_{1-42}$ and its significance. Human $A\beta_{1-42}$ rapidly increased intracellular Zn^{2+}, which was determined with intracellular ZnAF-2, in dentate granule cells, 5 min after injection of $A\beta_{1-42}$ (25 μM, 1 μl) into the dentate gyrus, while rat $A\beta_{1-42}$ did not increase intracellular Zn^{2+}. *In vivo* perforant pathway LTP was attenuated under pre-perfusion with 5 nM human $A\beta_{1-42}$ in artificial cerebrospinal fluid (ACSF) containing 10 nM Zn^{2+}, recapitulating the concentration of extracellular Zn^{2+}, but not with 5 nM rat $A\beta_{1-42}$ in ACSF containing 10 nM Zn^{2+}. The present study suggests that rat $A\beta_{1-42}$ has lower affinity for extracellular Zn^{2+} than human $A\beta_{1-42}$ and does not capture Zn^{2+} in the extracellular compartment, resulting in no significant effect on cognitive activity of rat even in the range of very low nanomolar concentrations of endogenous $A\beta_{1-42}$.

1. Introduction

Alzheimer's disease (AD), a progressive neurodegenerative disorder, is the most common form of dementia and has a preclinical phase of 20–30 years before clinical onset (Nestor et al., 2004; Querfurth and LaFerla, 2010). Amyloid-β (Aβ), a constituively-generated peptide, accumulation in the brain is the hallmark pathology of AD and is believed to play an upstream role in AD pathogenesis. Through mechanisms that are uncertain, endogenous Aβ can induce synapse dysfunction and contribute to cognitive decline in the pre-dementia stage of AD (Perrin et al., 2009a, b; Kepp, 2016).

Aβ is secreted into extracellular space after a sequential cleavage of amyloid precursor protein (APP) (Querfurth and LaFerla, 2010) and is normally produced in the brain, where the concentration has been estimated to be in the picomolar range in rodents (Cirrito et al., 2003). $A\beta_{1-40}$ and $A\beta_{1-42}$ are the two most abundant isoforms, and $A\beta_{1-40}$ is approximately 10 times as abundant as $A\beta_{1-42}$ in biological fluids (Schoonenboom et al., 2005). Importantly, $A\beta_{1-42}$ far more readily forms aggregates and is more neurotoxic than $A\beta_{1-40}$ (Mucke et al., 2000). Soluble $A\beta_{1-42}$ oligomers that are strong synaptotoxic molecules induce synaptic dysfunction and cognitive decline in AD (Walsh et al., 2002; Selkoe, 2008).

During the last few decades, transgenic mouse models have been developed for mimicing a range of AD-related pathologies. Although none of the models fully replicates the human disease, the models have been a key feature in translational research, providing important insights into the AD pathophysiology (Lithner et al., 2011). Transgenic rat models may offer distinctive advantages over mice. Rats are genetically, physiologically, and morphologically closer to humans. Importantly, the rat has a well-characterized, rich behavioral performance (Do Carmo and Cuello, 2013). On the other hand, much less attention has been paid to murine Aβ than human Aβ because mice and rats do not develop dementia and murine Aβ neurotoxicity is poorly understood. However, it is important to understand murine Aβ neurotoxicity when human Aβ neurotoxicity is evaluated in the normal mice and rats, especially in the range from high picomolar to very low nanomolar concentrations.

Zn^{2+} has been implicated in the AD pathogenesis by inducing human Aβ oligomerization (Bush et al., 1994; Bush, 2013; Adlard and Bush, 2018). We have been reported that human $A\beta_{1-42}$, unlike human $A\beta_{1-40}$, takes Zn^{2+} as a cargo into dentate granule cells in the normal rat brain, which causes cognitive decline *via* impairment of LTP

* Corresponding author.
E-mail address: takedaa@u-shizuoka-ken.ac.jp (A. Takeda).

https://doi.org/10.1016/j.neuro.2019.01.005
Received 21 September 2018; Received in revised form 17 January 2019; Accepted 17 January 2019
Available online 18 January 2019
0161-813X/

Fig. 1. Aβ peptide sequences, Potential zinc-binding sites are shown in bold black letters and the sequences associated with β-sheet structures are underlined with dots. Three amino acid residues underlined in murine $Aβ_{1–42}$ are different from human $Aβ_{1–42}$.

induction (Takeda et al., 2014, 2017, 2018). Here we test whether rat $Aβ_{1–42}$ takes Zn^{2+} as a cargo into dentate granule cells, resulting in cognitive decline (Fig. 1).

2. Materials and methods

2.1. Animals and chemicals

Male Wistar rats (7–9 weeks of age) were purchased from Japan SLC (Hamamatsu, Japan). Rats were housed under the standard laboratory conditions (23 ± 1 °C, 55 ± 5% humidity) and had access to tap water and food *ad libitum*. All the experiments were performed in accordance with the Guidelines for the Care and Use of Laboratory Animals of the University of Shizuoka that refer to the American Association for Laboratory Animals Science and the guidelines laid down by the NIH (NIH Guide for the Care and Use of Laboratory Animals) in the USA. The Ethics Committee for Experimental Animals in the University of Shizuoka has approved this work.

Synthetic human $Aβ_{1–42}$ and rat $Aβ_{1–42}$ were purchased from ChinaPeptides (Shanghai, China) and Bachem AG (Bubendorf, Swiss Confederation). Aβ was dissolved in saline and used immediately when the experiments were performed. ZnAF-2DA ($K_d = 2.7 \times 10^{-9}$ M for zinc), a membrane-permeable zinc indicator was kindly supplied from Sekisui Medical Co., LTD (Hachimantai, Japan). ZnAF-2DA is taken up into the cells through the cell membrane and is hydrolyzed by esterase in the cytosol to yield ZnAF-2, which cannot permeate the cell membrane (Hirano et al., 2002; Ueno et al., 2002). Calcium Orange AM, a membrane-permeable calcium indicator, was purchased from Molecular Probes, Inc. (Eugene, OR). These fluorescence indicators were dissolved in dimethyl sulfoxide (DMSO) and then diluted to artificial cerebrospinal fluid (ACSF) containing 119 mM NaCl, 2.5 mM KCl, 1.3 mM $MgSO_4$, 1.0 mM NaH_2PO_4, 2.5 mM $CaCl_2$, 26.2 mM $NaHCO_3$, and 11 mM D-glucose (pH 7.3).

2.2. In vivo LTP

Male rats were anesthetized with chloral hydrate (400 mg/kg) and placed in a stereotaxic apparatus. A bipolar stimulating electrode and a monopolar recording electrode made of tungsten wire attached to a microdialysis probe (AtmosLM™, 1000 kDa cutoff, outer diameter 0.44 mm, Eicom Co., Kyoto) were positioned stereotactically so as to selectively stimulate the perforant pathway while recording under local perfusion with agents in ACSF [127 mM NaCl, 2.5 mM KCl, 0.9 mM $MgCl_2$, 1.0 mM NaH_2PO_4, 1.3 mM $CaCl_2$, 21 mM $NaHCO_3$, and 3.4 mM D-glucose (pH 7.3)] at the rate of 1.0 μl/min in the dentate gyrus. The electrode stimulating the perforant pathway was positioned 8.0 mm posterior to the bregma, 4.5 mm lateral, 3.0–3.5 mm inferior to the dura. The recording electrode was implanted ipsilaterally 4.0 mm posterior to the bregma, 2.3–2.5 mm lateral and 3.0–3.5 mm inferior to the dura. All the stimuli were biphasic square wave pulses (200 μs width) and their intensities were set at the current that evoked 40% of the maximum population spike (PS) amplitude. Test stimuli (0.05 Hz) were delivered at 20 s intervals to monitor PS amplitude.

At the beginning of the experiments, input/output curves were generated by systematic variation of the stimulus current (0.1–1.0 mA) to evaluate synaptic potency. After stable baseline recording for at least 30 min, agents were added to the ACSF perfusate before LTP induction. LTP was induced by delivery of high-frequency stimulation (HFS; 10 trains of 20 pulses at 200 Hz separated by 1 s) and recorded for 60 min. Judging from the PS amplitude, in the present study, it is estimated that LTP was induced at the non-zincergic medial perforant pathway-DGC synapses (Sindreu et al., 2003). When the medial perforant pathway is electrically stimulated, it produces a characteristic waveform of evoked field excitatory postsynaptic potential (fEPSP) superimposed by a PS (Fukazawa et al., 2003). PS amplitudes (test frequency: 0.05 Hz) were averaged over 120-second intervals and expressed as percentages of the mean PS amplitude measured during the 30-min baseline recordings, which was expressed as 100%. PS amplitudes for the last 10 min were also averaged and represented as the magnitude of LTP.

2.3. In vivo intracellular Zn^{2+} imaging

According to the procedure described above, injection cannulae were bilaterally inserted into the dentate granule cell layer of anesthetized rats. Thirty minutes later, 25 μM $Aβ_{1–42}$ in ACSF containing 100 μM ZnAF-2DA was bilaterally injected *via* injection cannulae at the rate of 0.25 μl/min for 4 min. Five minutes later, the brain was quickly removed and immersed in ice-cold choline-ACSF containing 124 mM choline chloride, 2.5 mM KCl, 2.5 mM $MgCl_2$, 1.25 mM NaH_2PO_4, 0.5 mM $CaCl_2$, 26 mM $NaHCO_3$, and 10 mM glucose (pH 7.3) to suppress excessive neuronal excitation. Horizontal hippocampal slices (400 μm) were prepared in ice-cold choline-ACSF using a vibratome ZERO-1 (Dosaka Kyoto, Japan) in an ice-cold choline-ACSF. Slices were then maintained in ACSF at 25 °C for at least 30 min. All solutions used in the experiments were continuously bubbled with 95% O_2 and 5% CO_2.

The hippocampal slices were transferred to a chamber filled with ACSF, loaded with 2 μM Calcium Orange AM in ACSF for 30 min to identify hippocampal regions, and then rinsed in ACSF for 10 min. The hippocampal slices were transferred to a recording chamber filled with ACSF. The fluorescence of ZnAF-2 (laser, 488.4 nm; emission, 500–550 nm) and calcium orange (laser, 561.4 nm; emission, 570–620 nm) was measured with a confocal laser-scanning microscopic system (Nikon A1 confocal microscopes, Nikon Corp.).

2.4. Data analysis

For multiple comparisons, differences between treatments were assessed by one-way ANOVA followed by post hoc testing using the Tukey's test (the statistical software, GraphPad Prism 5). A value of $p < 0.05$ was considered significant. Data were expressed as means ± standard error.

3. Results

Human $Aβ_{1–42}$ rapidly increases intracellular Zn^{2+} in dentate granule cells after injection of $Aβ_{1–42}$ (25 μM, 1 μl) into the dentate gyrus (Takeda et al., 2014). $Aβ_{1–42}$ captures Zn^{2+} in the extracellular compartment and both levels of $Aβ_{1–42}$ and Zn^{2+} are increased in dentate granule cells, resulting in cognitive decline *via* attenuated LTP. In contrast, human $Aβ_{1-40}$ does not increase intracellular Zn^{2+}, probably because of no formation of a Zn-$Aβ_{1-40}$ complex in the extracellular compartment (Takeda et al., 2017). The difference in affinity of Aβ to Zn^{2+} in the extracellular compartment may be linked with Aβ-mediated attenuation of *in vivo* perforant pathway LTP under the local perfusion with 5 nM Aβ in ACSF containing 10 nM Zn^{2+}, recapitulating the concentration of extracellular Zn^{2+} (Frederickson et al., 2006); $Aβ_{1–42}$ attenuates LTP, while $Aβ_{1–40}$ does not attenuate LTP (Takeda et al., 2017). In the present study, $Aβ_{1–42}$-induced attenuation of LTP was rescued by adding CaEDTA, an extracellular Zn^{2+} chelator to ACSF perfusate (control, 244 ± 20%; Aβ, 175 ± 17%; Aβ + CaEDTA,

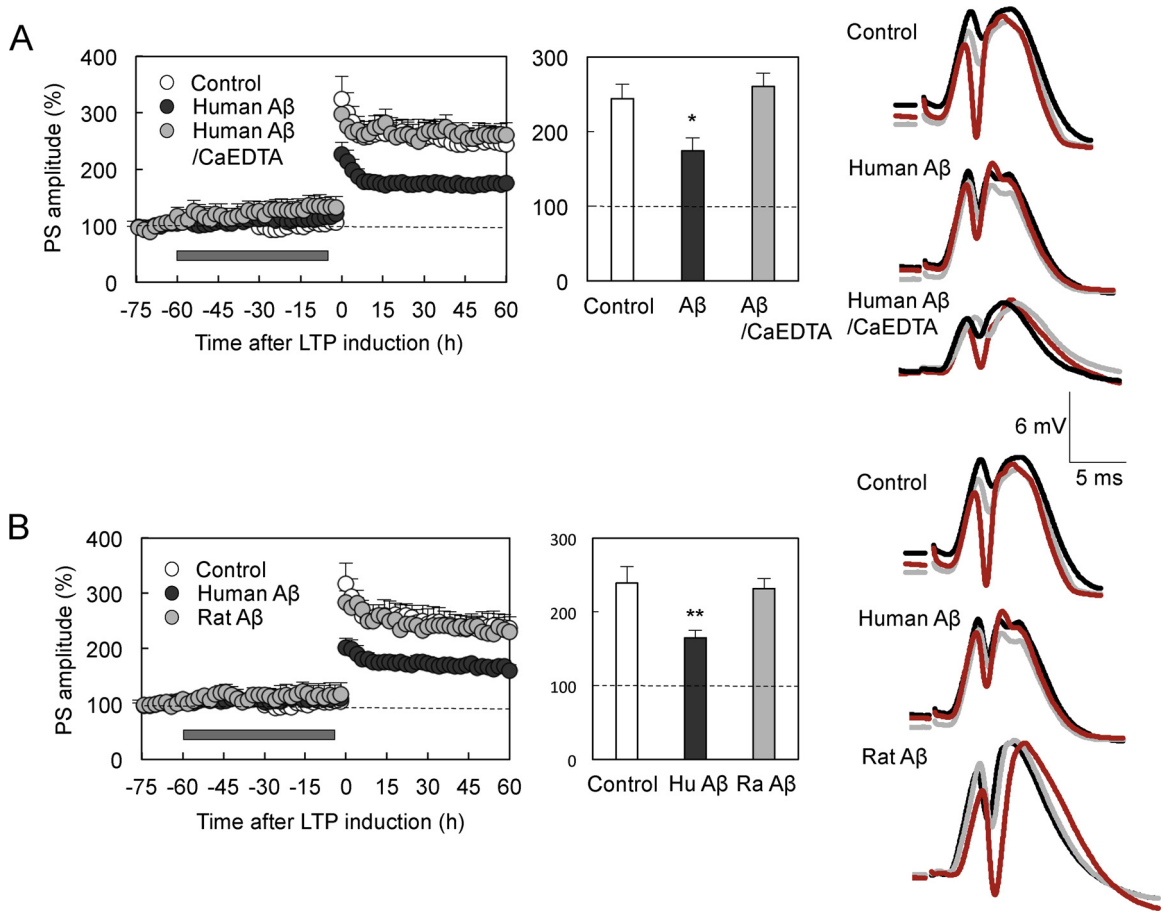

Fig. 2. LTP is attenuated in the presence of human $A\beta_{1-42}$, but not rat $A\beta_{1-42}$, (A) LTP was induced under pre-perfusion with 5 nM human $A\beta_{1-42}$ + 10 nM $ZnCl_2$ (n = 8) and 5 nM human $A\beta_{1-42}$ + 10 nM $ZnCl_2$ + 1 mM CaEDTA (n = 5) in ACSF. The bar represents the perfusion period (left). Each bar and line (mean ± SEM) represents the averaged PS amplitude of the last 10 min. (middle). Representative fEPSP with PS recordings at the time −70 min (grey), -30 min (black) and 50–60 min (red) are shown (right). *, $p < 0.05$, vs. control (n = 11). (B) LTP was induced under pre-perfusion with 5 nM human $A\beta_{1-42}$ + 10 nM $ZnCl_2$ (n = 8) and 5 nM rat $A\beta_{1-42}$ + 10 nM $ZnCl_2$ (n = 5) in ACSF in the same manner. The bar represents the perfusion period (left). Each bar and line (mean ± SEM) represents the averaged PS amplitude of the last 10 min. (middle). Representative fEPSP with PS recordings at the time −70 min (grey), -30 min (black) and 50–60 min (red) are shown (right). *, $p < 0.05$, vs. control (n = 10) (For interpretation of the references to colour in this figure legend, the reader is referred to the web version of this article).

261 ± 17%) (Fig. 2A).

Because estimated amino acid residues bound to human $A\beta_{1-42}$ are different in murine $A\beta_{1-42}$ (Fig. 1), it is estimated that affinity of Aβ to Zn^{2+} is different between human and murine $A\beta_{1-42}$, potentially resulting in differential synapse toxicity. Murine $A\beta_{1-42}$ did not attenuate LTP under the same perfusion condition (control, 240 ± 23%; human Aβ, 165 ± 10%; rat Aβ, 232 ± 14%) (Fig. 2B).

$A\beta_{1-42}$-mediated Zn^{2+} dynamics was compared after injection of human and murine $A\beta_{1-42}$ in saline containing ZnAF-2DA into the dentate gyrus. Human $A\beta_{1-42}$ increased intracellular Zn^{2+} levels in the dentate granule cell layer, which were detected with intracellular ZnAF-2, in only the injected area 5 min after injection (Fig. 3). In contrast, murine $A\beta_{1-42}$ did not increase intracellular Zn^{2+} levels in the dentate granule cell layer, suggesting that murine $A\beta_{1-42}$ does not capture Zn^{2+} in the extracellular compartment.

4. Discussion

Synaptic vesicle release may be the primary mediator of dynamic changes in extracellular Aβ levels, which are independent of changes in amyloid-β precursor protein (APP) processing, and is linked with synaptic activity (Cirrito et al., 2005). In normal young mice, endogenous $A\beta_{1-42}$ is involved in learning and memory *via* facilitating hippocampal LTP (Morley et al., 2010). Puzzo et al. (2011) report that both antirodent Aβ antibody and siRNA against murine APP attenuate LTP as well as contextual fear memory and reference memory. These negative effects are rescued by the addition of human $A\beta_{1-42}$, suggesting that endogenously produced Aβ is required for normal LTP and memory. Taken together, it is likely that $A\beta_{1-42}$ supports LTP and memory at picomolar concentrations under physiological conditions (Puzzo et al., 2012). In contrast, human $A\beta_{1-42}$ affects hippocampal LTP in murine in the concentration range of more than 1 nM (Rammes et al., 2011), while the action of murine $A\beta_{1-42}$ in LTP is unknown.

Because human $A\beta_{1-42}$ induces cognitive decline *via* increase in intracellular Zn^{2+} in dentate granule cells after injection of human $A\beta_{1-42}$ into the rat dentate gyrus (Takeda et al., 2014, 2017, 2018), here we compared ability for extracellular Zn^{2+} influx into dentate granule cells of rats between human and rat $A\beta_{1-42}$. Human $A\beta_{1-42}$ rapidly increases intracellular Zn^{2+} in dentate granule cells after injection of $A\beta_{1-42}$ (25 μM, 1 μl) into the dentate gyrus, which attenuates LTP (Takeda et al., 2014), but not after injection of $A\beta_{1-42}$ (12.5 μM, 1 μl) into the dentate gyrus, which does not attenuate LTP (Takeda et al., 2018). Thus, the former dose was used to compare ability for extracellular Zn^{2+} influx. Under this condition, rat $A\beta_{1-42}$ did not increase intracellular Zn^{2+} in dentate granule cells, unlike human $A\beta_{1-42}$. Human Aβ has self-aggregation ability and Aβ fibrils are main components of Aβ plaques, a pathological hallmark of AD (Querfurth and LaFerla, 2010). Human Aβ is bound to Zn^{2+} *via* histidine residues

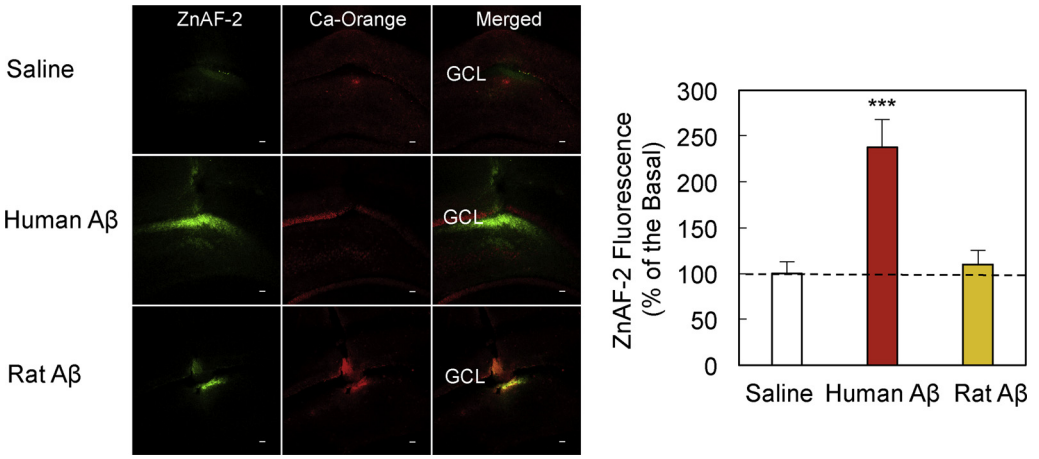

Fig. 3. *In vivo* $A\beta_{1-42}$-mediated intracellular Zn^{2+} dynamics in the dentate gyrus, Intracellular Zn^{2+} images were determined in the dentate gyrus 5 min after bilateral injection of 25 μM human $A\beta_{1-42}$ (n = 18) and 25 μM rat $A\beta_{1-42}$ (n = 12) in ACSF into the dentate gyrus. Scale bar, 50 μm (left). Intracellular Zn^{2+} level in the dentate granule cell layer determined with intracellular ZnAF-2 is represented by the ratio to the control (saline) (n = 21) without $A\beta_{1-42}$ expressed as 100% (right). ***, $p < 0.001$, vs. control.

(Fig. 1) and the K_d values of Zn^{2+} to $A\beta_{1-40}$ are in the range of 0.1–60 μM (Tõugu et al., 2008). On the other hand, it has been reported that formation and propagation of misfolded aggregates of $A\beta_{1-42}$ contribute to AD pathogenesis rather than $A\beta_{1-40}$, although structure of misfolded $A\beta_{1-42}$ is poorly understood (Ahmed et al., 2010). C-Terminal carboxylate anion of $A\beta_{1-42}$ constructs the C-terminal hydrophobic core, which accelerates neurotoxic oligomerization (Masuda et al., 2009). C-Terminal Ala42 that is absent in $A\beta_{1-40}$ constructs a salt bridge with Lys28 to create a self-recognition molecular switch, which is the $A\beta_{1-42}$-selective self-replicating amyloid-propagation machinery (Xiao et al., 2015). C-Terminal β-sheet structure may be indirectly involved in the affinity of human $A\beta_{1-42}$ for Zn^{2+}. The aggregating property of human $A\beta_{1-42}$ is rapidly promoted in the presence of Zn^{2+}, resulting in much higher affinity of $A\beta_{1-42}$ to Zn^{2+} than $A\beta_{1-40}$, and the K_d values of Zn^{2+} to $A\beta_{1-42}$ are in the range of 3–30 nM (Takeda et al., 2017). The amino acid sequence, which constructs β-sheet structure, is the same between human and rat $A\beta_{1-42}$, while amino acid residues including three histidine residues, which are estimated to be interacted with Zn^{2+}, are different between them (Watt et al., 2010) (Fig. 1), resulting in lower affinity of rat $A\beta_{1-42}$ to Zn^{2+} than human $A\beta_{1-42}$.

$A\beta_{1-42}$ captures extracellular Zn^{2+} at the concentration of 5 nM and the formation of Zn-$A\beta_{1-42}$ in the extracellular compartment is essential for Zn-$A\beta_{1-42}$ uptake into dentate granule cells, followed by attenuated LTP induction and cognitive decline (Takeda et al., 2017), while $A\beta_{1-40}$ has no effect on LTP induction, probably because of no formation of a Zn-$A\beta_{1-40}$ complex under extracellular Zn^{2+} concentration (˜10 nM). Judging from no increase in intracellular Zn^{2+} after injection of rat $A\beta_{1-42}$ into the dentate gyrus, it is possible that rat $A\beta_{1-42}$, unlike human $A\beta_{1-42}$, is not taken up into dentate granule cell at the concentration of 5 nM. *In vivo* perforant pathway LTP was attenuated under pre-perfusion with 5 nM human $A\beta_{1-42}$ in ACSF containing 10 nM Zn^{2+}, but not with 5 nM rat $A\beta_{1-42}$ in ACSF containing 10 nM Zn^{2+}. Human $A\beta_{1-42}$-induced attenuation of LTP was rescued in the presence of extracellular Zn^{2+} chelator (CaEDTA). In the dentate gyrus exposed to human $A\beta_{1-42}$, human $A\beta_{1-42}$ stain, which was determined by Aβ monoclonal antibody, 4G8, was preferentially observed in the dentate granule cell layer and was often observed around the nuclei of dentate granule cells. At this time, intracellular Zn^{2+} levels, which were determined by ZnAF-2DA, were increased in an extended area including the dentate granule cell layer and the hilus (Takeda et al., 2017), as shown in the ZnAF-2 image with human $A\beta_{1-42}$ in Fig. 2. Judging from the evidence, it is estimated that Zn^{2+} preferentially accumulates in dentate granule cells in the dentate gyrus because Zn^{2+} accumulation occurs human $A\beta_{1-42}$-dependently, resulting in attenuation of *in vivo* perforant pathway LTP (Takeda et al., 2017). In the dentate gyrus exposed to rat $A\beta_{1-42}$, on the other hand, the data that intracellular Zn^{2+} levels was not significantly increased compared to the control exposed to vehicle suggest that extracellular Zn^{2+} is not captured with rat $A\beta_{1-42}$. Therefore, Zn^{2+} accumulation does not occur in cells exposed to rat $A\beta_{1-42}$ unlike cells exposed to human $A\beta_{1-42}$.

Rat $A\beta_{1-42}$ reduces the proneness to form β-sheet structures and aggregated fibrils, and decreases the cytotoxicity, in comparison with human $A\beta_{1-42}$ (Lv et al., 2013). On the other hand, rat Aβ peptides have the capacity to produce amyloid deposits that are morphologically similar to deposits observed in human AD (Xu et al., 2015)

In conclusion, the present study suggests that rat $A\beta_{1-42}$ has lower affinity for extracellular Zn^{2+} than human $A\beta_{1-42}$ and does not capture Zn^{2+} in the extracellular compartment, resulting in no increase in intracellular Zn^{2+}, unlike human $A\beta_{1-42}$. Human $A\beta_{1-42}$ attenuates *in vivo* perforant pathway LTP even at the concentration of 0.5 nM in the presence of extracellular Zn^{2+} (Takeda et al., 2017), while Rat $A\beta_{1-42}$ has no effect on it at the concentration of 5 nM. Therefore, mice and rats are applicable to study of human $A\beta_{1-42}$ synaptotoxicity even in the range of < 1 nM.

Conflicts of interest

There are no conflicts to declare.

References

Adlard, P.A., Bush, A.I., 2018. Metals and Alzheimer's disease: how far have we come in the clinic? J. Alzheimers Dis. 62 (3), 1369–1379.
Ahmed, M., Davis, J., Aucoin, D., Sato, T., Ahuja, S., Aimoto, S., Elliott, J.I., Van Nostrand, W.E., Smith, S.O., 2010. Structural conversion of neurotoxic amyloid-beta (1-42) oligomers to fibrils. Nat. Struct. Mol. Biol. 17, 561–567.
Bush, A.I., 2013. The metal theory of Alzheimer's disease. J. Alzheimers Dis. 33, S277–281.
Bush, A.I., Pettingell, W.H., Multhaup, G., d Paradis, M., Vonsattel, J.P., Gusella, J.F., Beyreuther, K., Masters, C.L., Tanzi, R.E., 1994. Rapid induction of Alzheimer A beta amyloid formation by zinc. Science 265, 1464–1467.
Cirrito, J.R., May, P.C., O'Dell, M.A., Taylor, J.W., Parsadanian, M., Cramer, J.W., Audia, J.E., Nissen, J.S., Bales, K.R., Paul, S.M., DeMattos, R.B., Holtzman, D.M., 2003. *In vivo* assessment of brain interstitial fluid with microdialysis reveals plaque-associated changes in amyloid-β metabolism and half-life. J. Neurosci. 23, 8844–8853.
Cirrito, J.R., Yamada, K.A., Finn, M.B., Sloviter, R.S., Bales, K.R., May, P.C., Schoepp, D.D., Paul, S.M., Mennerick, S., Holtzman, D.M., 2005. Synaptic activity regulates interstitial fluid amyloid-beta levels in vivo. Neuron 48, 913–922.
Do Carmo, S., Cuello, A.C., 2013. Modeling Alzheimer's disease in transgenic rats. Mol. Neurodegener. 8, 37. https://doi.org/10.1186/1750-1326-8-37.
Frederickson, C.J., Giblin, L.J., Krezel, A., McAdoo, D.J., Muelle, R.N., Zeng, Y., Balaji, R.V., Masalha, R., Thompson, R.B., Fierke, C.A., Sarvey, J.M., Valdenebro, M., Prough, D.S., Zornow, M.H., 2006. Concentrations of extracellular free zinc (pZn)e in the central nervous system during simple anesthetization, ischemia and reperfusion. Exp. Neurol. 198, 285–293.
Fukazawa, Y., Saitoh, Y., Ozawa, F., Ohta, Y., Mizuno, K., Inokuchi, K., 2003. Hippocampal LTP is accompanied by enhanced F-actin content within the dendritic spine that is essential for late LTP maintenance in vivo. Neuron 38, 447–460.
Kepp, K.P., 2016. Alzheimer's disease due to loss of function: a new synthesis of the available data. Prog. Neurobiol. 143, 36–60.
Lithner, C.U., Hedberg, M.M., Nordberg, A., 2011. Transgenic mice as a model for Alzheimer's disease. Curr. Alzheimer Res. 8, 818–831.
Lv, X., Li, W., Luo, Y., Wang, D., Zhu, C., Huang, Z.X., Tan, X., 2013. Exploring the

differences between mouse mAβ(1-42) and human hAβ(1-42) for Alzheimer's disease related properties and neuronal cytotoxicity. Chem. Commun. (Camb.) 49, 5865–5867.
Masuda, Y., Uemura, S., Ohashi, R., Nakanishi, A., Takegoshi, K., Shimizu, T., Shirasawa, T., Irie, K., 2009. Identification of physiological and toxic conformations in Abeta42 aggregates. Chembiochem 10, 287–295.
Morley, J.E., Farr, S.A., Banks, W.A., Johnson, S.N., Yamada, K.A., Xu, L., 2010. A physiological role for amyloid beta protein: enhancement of learning and memory. J. Alzheimer Dis. 19, 441–449.
Mucke, L., Masliah, E., Yu, G.Q., Mallory, M., Rockenstein, E.M., Tatsuno, G., 2000. High-level neuronal expression of abeta 1-42 in wild-type human amyloid protein precursor transgenic mice: synaptotoxicity without plaque formation. J. Neurosci. 20, 4050–4058.
Nestor, P.J., Scheltens, P., Hodges, J.R., 2004. Advances in the early detection of Alzheimer's disease. Nat. Med. 10, S34–S41.
Perrin, R.J., Fagan, A.M., Holtzman, D.M., 2009a. Multimodal techniques for diagnosis and prognosis of Alzheimer's disease. Nature 461, 916–922.
Perrin, R.J., Fagan, A.M., Holtzman, D.M., 2009b. Multimodal techniques for diagnosis and prognosis of Alzheimer's disease. Nature 461, 916–922.
Puzzo, D., Privitera, L., Fa', M., Staniszewski, A., Hashimoto, G., Aziz, F., Sakurai, M., Ribe, E.M., Troy, C.M., Mercken, M., Jung, S.S., Palmeri, A., Arancio, O., 2011. Endogenous amyloid-β is necessary for hippocampal synaptic plasticity and memory. Ann. Neurol. 69, 819–830.
Puzzo, D., Privitera, L., Palmeri, A., 2012. Hormetic effect of amyloid-β peptide in synaptic plasticity and memory. Neurobiol. Aging 33 (1484), e15–24.
Querfurth, H.W., LaFerla, F.M., 2010. Alzheimer's disease. N. Engl. J. Med. 362, 329–344.
Rammes, G., Hasenjäger, A., Sroka-Saidi, K., Deussing, J.M., Parsons, C.G., 2011. Therapeutic significance of NR2B-containing NMDA receptors and mGluR5 metabotropic glutamate receptors in mediating the synaptotoxic effects of β-amyloid oligomers on long-term potentiation (LTP) in murine hippocampal slices. Neuropharmacology 60, 982–990.
Schoonenboom, N.S., Mulder, C., Van Kamp, G.J., Mehta, S.P., Scheltens, P., Blankenstein, M.A., Mehta, P.D., 2005. Amyloid beta 38, 40, and 42 species in cerebrospinal fluid: more of the same? Ann. Neurol. 58, 139–142.
Selkoe, D.J., 2008. Soluble oligomers of the amyloid β-Protein impair synaptic plasticity and behavior. Behav. Brain Res. 192, 106–113.
Sindreu, C.B., Varoqui, H., Erickson, J.D., Pérez-Clausell, J., 2003. Boutons containing vesicular zinc define a subpopulation of synapses with low AMPAR content in rat hippocampus. Cereb. Cortex 13, 823–829.
Takeda, A., Nakamura, M., Fujii, H., Uematsu, C., Minamino, T., Adlard, P.A., Bush, A.I., Tamano, H., 2014. Amyloid β-mediated Zn^{2+} influx into dentate granule cells transiently induces a short-term cognitive deficit. PLoS One 9, e115923.
Takeda, A., Tamano, H., Tempaku, M., Sasaki, M., Uematsu, C., Sato, S., Kanazawa, H., Datki, Z.L., Adlard, P.A., Bush, A.I., 2017. Extracellular Zn^{2+} is essential for amyloid β1-42-induced cognitive decline in the normal brain and its rescu. J. Neurosci. 37, 7253–7262.
Takeda, A., Tamano, H., Hashimoto, W., Kobuchi, S., Suzuki, H., Murakami, T., Tempaku, M., Koike, Y., Adlard, P.A., Bush, A.I., 2018. Novel defense by metallothionein induction against cognitive decline: from amyloid β1-42-induced excess Zn^{2+} to functional Zn^{2+} deficiency. Mol. Neurobiol. 55, 7775–7788.
Tõugu, V., Karafin, A., Palumaa, P., 2008. Binding of zinc(II) and copper(II) to the full-length Alzheimer's amyloid-beta peptide. J. Neurochem. 104, 1249–1259.
Walsh, D.M., Klyubin, I., Fadeeva, J.V., Cullen, W.K., Anwyl, R., Wolfe, M.S., Rowan, M.J., Selkoe, D.J., 2002. Naturally secreted oligomers of amyloid β protein potently inhibit hippocampal long-term potentiation in vivo. Nature 416, 535–539.
Watt, N.T., Whitehouse, I.J., Hooper, N.M., 2010. The role of zinc in Alzheimer's disease. Int. J. Alzheimers Dis. 2011, 971021.
Xiao, Y., Ma, B., McElheny, D., Parthasarathy, S., Long, F., Hoshi, M., Nussinov, R., Ishii, Y., 2015. Aβ(1-42) fibril structure illuminates self-recognition and replication of amyloid in Alzheimer's disease. Nat. Struct. Mol. Biol. 22, 499–505.
Xu, G., Ran, Y., Fromholt, S.E., Fu, C., Yachnis, A.T., Golde, T.E., Borchelt, D.R., 2015. Murine Aβ over-production produces diffuse and compact Alzheimer-type amyloid deposits. Acta Neuropathol. Commun. 3, 72.